Hakim Ait Said[1,*]
Dr Massinissa Aissou[1],
Dr Hamou Nouri[1],
Pr Youcef Zebboudj[1]

J. Electrical Systems 10-4 (2014): 392-405

Regular paper

Effect of Wires Number on Corona Discharge of an Electrostatic Precipitators

Journal of Electrical Systems

This paper aims to analyze the behavoir of DC corona discharge in wires-to-planes electrostatic precipitators (ESPs) with effect of the wires number. The current-voltage characteristics, onset corona voltage, electric onset field, breakdown voltage, current density and the apparent mobility of the charge carriers are analyzed. The values of the current at the plane surface were the maximum beneath the wires which decreased when moving away from them. Experimental results show that discharge current is strongly affected by the wires number, general formula was developed by Meng can be apply in wires-to-planes system of an electrostatic precipitators. The Coopeman s model is reliable to determine the mobility of the charge carriers in this system.

Keywords: Corona Discharge, Electrostatic Precipitateur, Onset Corana Voltage, Apparent Mobility.

Article history: Received 10 June 2014, Received in revised form 5 September 2014, Accepted 15 September 2014

1. Introduction

The DC corona discharge has numerous applications, such as in electrostatic precipitation, generation of ozone, decomposition of toxic gases, ion sources for mass spectrometers, ionic wind blowers and many others [1-6]. The corona discharges between active (small radius of curvature) and passive (plane) electrodes are one of the more common low-temperature, non-equilibrium plasmas because they are easy to generate, stable at atmospheric pressure, operate at low currents (μA) and power consumption. The process of corona generation in the air at atmospheric conditions requires a non uniform electrical field, which can be obtained by the use of a small diameter wire electrode, energized from a high-voltage supply, and a metallic plate or cylinder, connected to the ground, which is designated as collecting electrode. The Industrial ESPs are used with success to reduce the emissions of smoke, fumes and dust, playing an important role to maintain a clean environment and to improve the air quality [7-10]. The configuration mostly used in electrostatic precipitation technique is the wires-to-planes. It consists of high-field parallel active wires located midway between the grounded plates (the collecting electrodes) where the gas flows through. The ions produced by the corona discharge near the wires charge the dust particles which are thus driven toward the collecting plates. The particle charges are neutralized and the particle is thus collected. Although the geometry is simple, there is a complex behavior of the gas flow [11-12]. The ions produced by the corona discharge drift along the electric field to the plate collector and due to collision with neutral air molecules, there is a momentum transfer to the flow by the electric field. The main objective of this investigation is to analyze the effect of the number of wires, which can vary from 1W-ESP to 8W-ESP, on both positive and negative DC corona discharges employed in wire-to-plane ESPs. In particular, the current-voltage characteristics, onset corona voltage, electric onset field, breakdown voltage, apparent mobility of the charge carriers and the current density are analyzed and discussed.

* Corresponding author: H. Ait Said, Laboratoire de Génie Electrique, Université A. Mira de Béjaïa, 06000 Béjaïa, Algérie, E-mail: hakimdoz@yahoo.fr
[1] Laboratoire de Génie Electrique, Université A. Mira de Béjaïa, 06000 Béjaïa, Algérie

2. Experimental methods

The figure 1 shows the experimental setup used in this study we propose to explain later in this section.

1.1 Geometric configuration

The system used consists of a nickel active electrode (1) (Anode) and a passive electrode (2) (Cathode). The active electrode is a small radius of curvature $r_0 = 0.2mm$ and the length of the wire $l = 200mm$, it is surrounded by an area of high field where ionization takes place then by a smaller area where the charged particles drift field. The gap between the wires and the collector$h = 50mm$, distance between two adjacent wires $2a = 40mm$. The measurement plane (2) and plane (3) are made of stainless steel. The number of wires n who made the active electrode is variable from 1wire to 8wires.

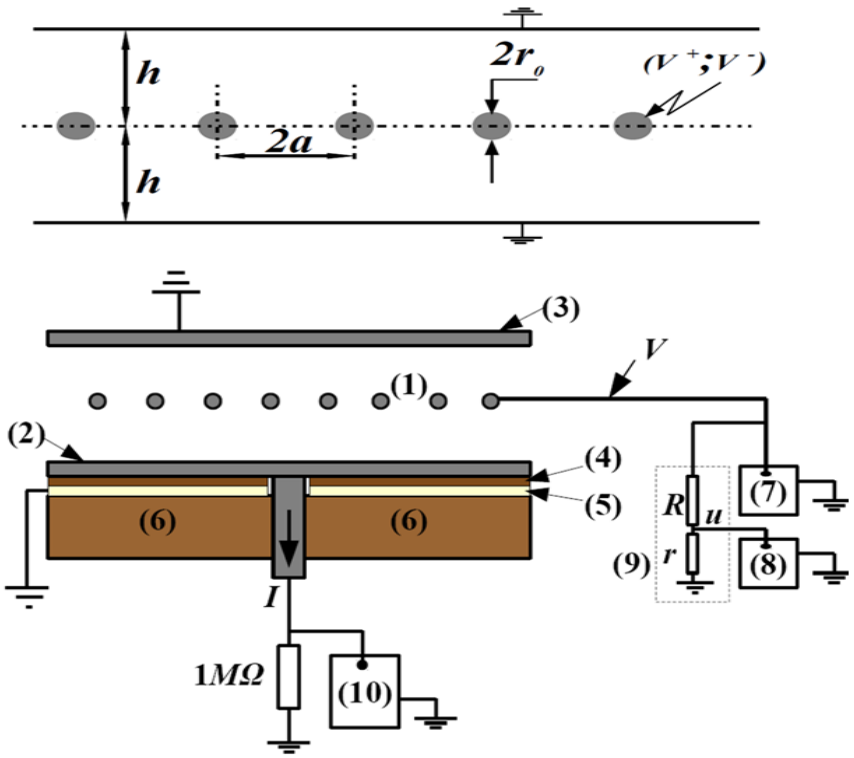

Fig. 1. Experimental setup.

1.2 Electrical measurements

The corona discharge is generated by applying an electric field; share a highly inhomogeneous due to the geometric configuration of the electrodes, and on the other hand high enough to produce a partial ionization of the gas. A high-voltage source (7) has been used to produce the positive or negative DC discharge. The active electrode (1) is connected to the DC high-voltage installation which has a voltage between 0 and $\pm$ 140 kV (7). The latter is provided after half-wave rectification made of a high voltage silicon diode capable of supporting a voltage of 270 kV, a smoothing capacitor 10 nF, resistance

$r = 250M\Omega$ and a damping resistor $R = 106k\Omega$, its role is to protect the diode from over-current. The original alternating voltage is generated by amplification of a variable low voltage applied to the primary of an elevator transformer whose secondary is connected to the diode. Measuring the DC voltage is performed using a voltmeter (8). The value of the discharge current is measured with a multimeter (10) with accuracy of the order mV.

3 Results and discussion

3.1 Current-voltage characteristics

The figures 2-3 show the waveforms of current / voltage characteristics in the case of 1W- ESP to 8W-ESP for both discharges. The behavior of the discharge is similar in eight ESP.

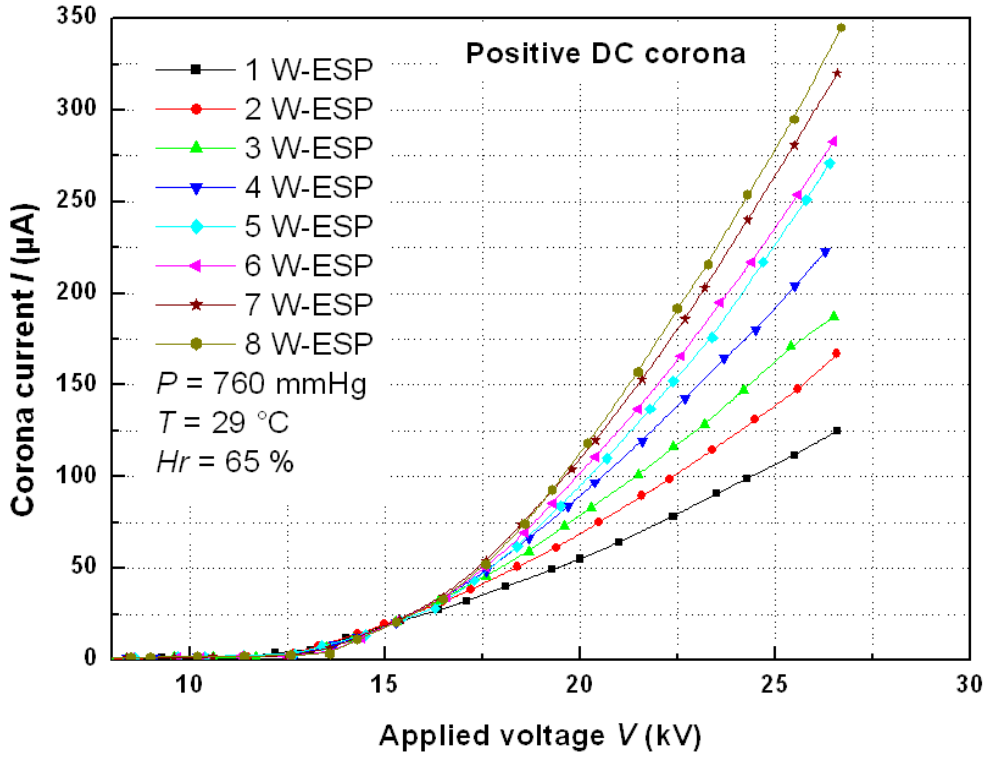

Fig. 2. Current-voltage characteristics for the DC positive corona.

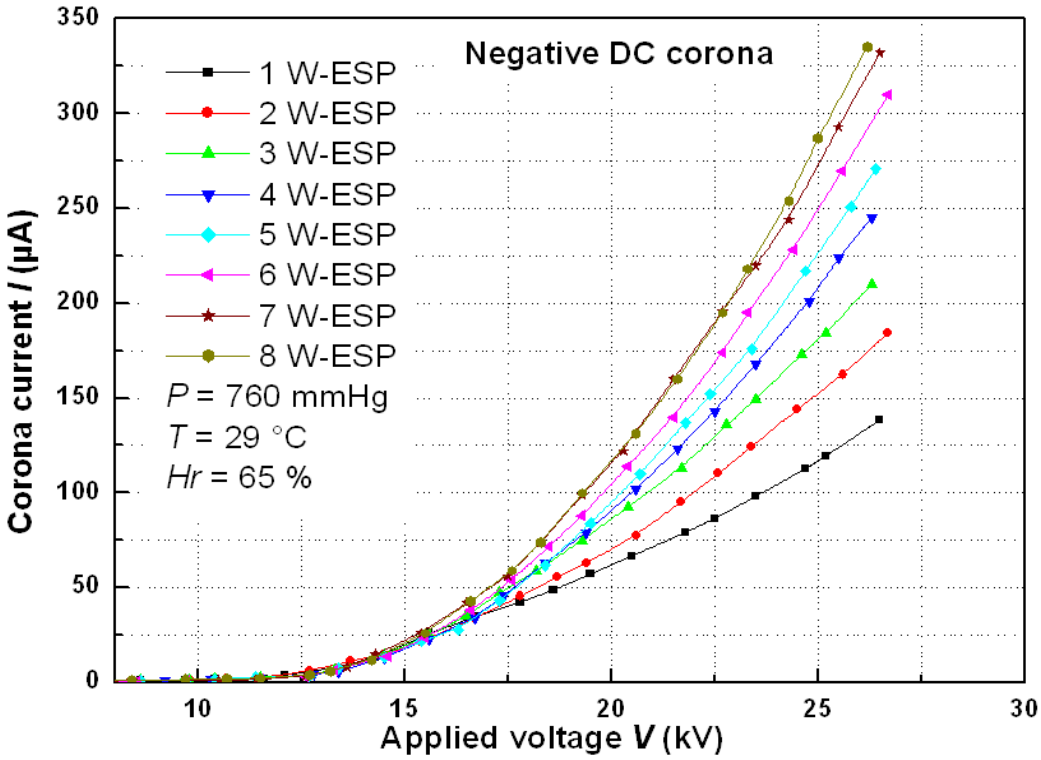

Fig. 3. Current-voltage characteristics for the DC negative corona.

The current gradually increases with the applied voltage when it exceeds a certain value (V_0) and that the gaseous medium until breakdown. The DC current through the inter-electrode gap is a nonlinear function of the applied voltage [13]. The measured characteristics follow the law of Townsend [14]. It is expressed by:

$$I = AV(V - V_0), \tag{1}$$

$$I = \frac{8\pi\varepsilon_0\mu * l}{R^2 \log\left({}^{R}/_{r_0}\right)} V(V - V_0), \tag{2}$$

Where I is the corona discharge current, V is the applied voltage, $V_0$is the discharge onset voltage for inner and outer electrodes of radius r_0 and R, l is the length of the wire, A is the constant depending on the electrode configuration, the temperature, pressure and gas composition, μ is the mobility of the ionic carriers resulting from the discharge and ε_0 permittivity. Other authors [15-17] have reported attempts to derive the law of Townsend for point-plane system. Research on the current-voltage characteristic of the discharge reported attempts to develop a model for the law of Townsend. Meng et al. [18] have recently developed an empirical formula, based on experimentation, the law of Townsend in the system point-plane:

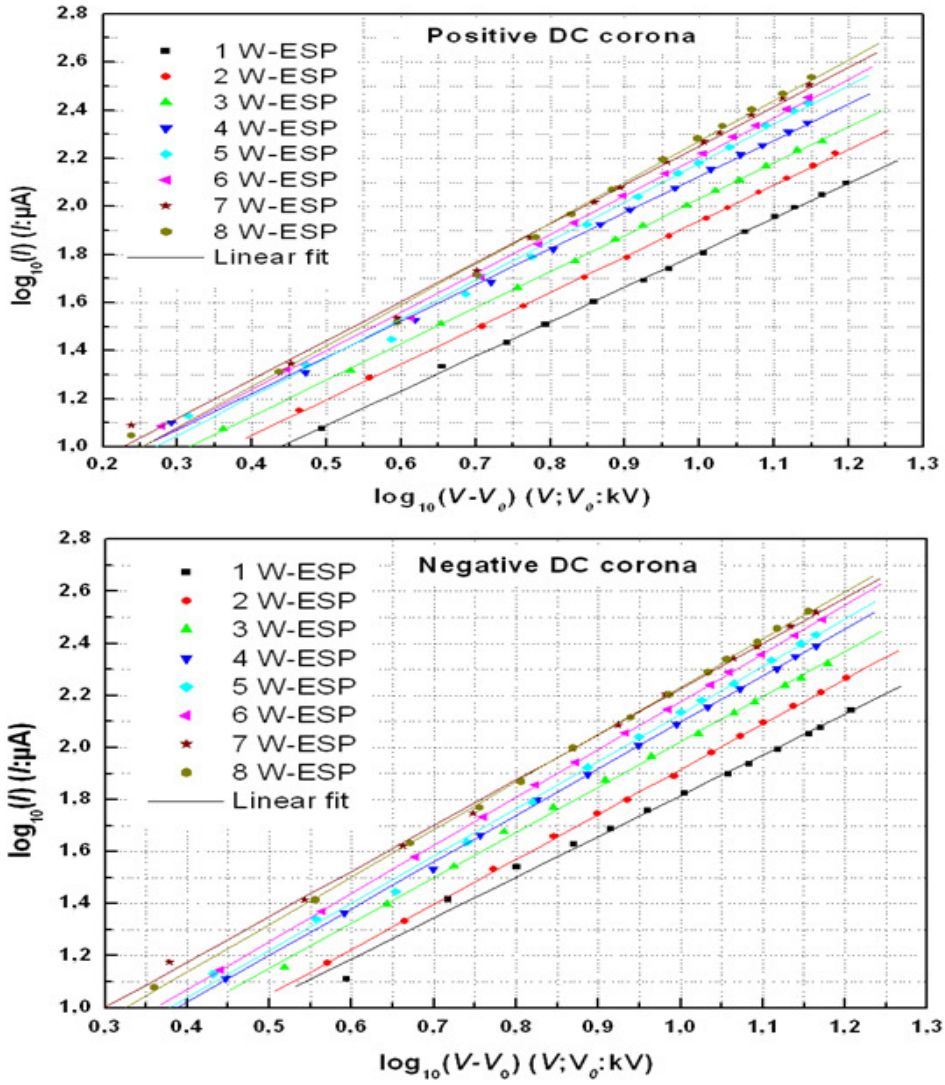

Fig. 4. The dependence of the current I on the voltage difference $(V - V_0)$ on a log scale.

$$I = K(V - V_0)^m \tag{3}$$

Where K is the dimensional constant and m is the parameter that falls in the range 1.5-2.0 and has a value of 1.6 for their study [19]. The main criticism of the law of Townsend suggested by the authors is that the parameter K and V_0 depends on the inter-electrode distance. The I-V characteristics of the corona discharge in systems 1W-EPS to 8W-EPS seem to follow proposed by Meng et al. [18] given by equation (3). To determine the exponent m, we use the logarithmic scale of the dependence of discharge current I of the voltage difference $(V - V_0)$ shown in figure 4. In our study, the values of the exponent m are given in Table 1.

The I-V characteristics measured when the wire in negative polarity are always higher than those measured in positive polarity, figure 5. In fact, the negative current values are higher than those positive for the same applied voltage. This is due to the existence of a difference

between the positive and negative inception voltage, also the mobility of negative ions is higher than that of positive ions.

Table 1. Results of exponent *m* for the postive and negative corona.

Wires number (n)	Exponent *m* (positive DC corona)	Exponent *m* (negative DC corona)
1 Wire	1.5	1.57
2 Wires	1.52	1.73
3 Wires	1.53	1.74
4 Wires	1.56	1.79
5 Wires	1.62	1.82
6 Wires	1.61	1.84
7 Wires	1.64	1.75
8 Wires	1.7	1.83

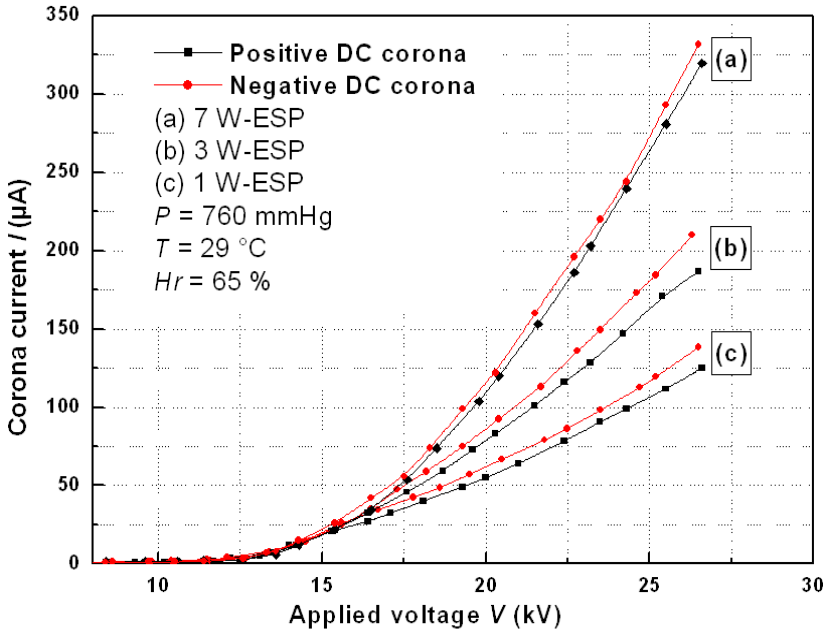

Fig. 5. Comparison the current-voltage characteristics for the postive and negative corona.

3.2 Effect of active electrode on electric onset voltage, electric onset field and breakdown voltage

We used the $(I^{1/2}) = f(V)$ function proposed by Frechette et al. [20] to determine the onset voltage V_0 and the onset field E_0 can be calculated by the following formula:

$$E_0 = \frac{V_0}{r_0 log(^d/_{r_0})} \quad (4)$$

Figures 6-7 show the influence of wires number forming the active electrode of an electrostatic precipitator on the onset voltage and the onset field of the corona discharge.

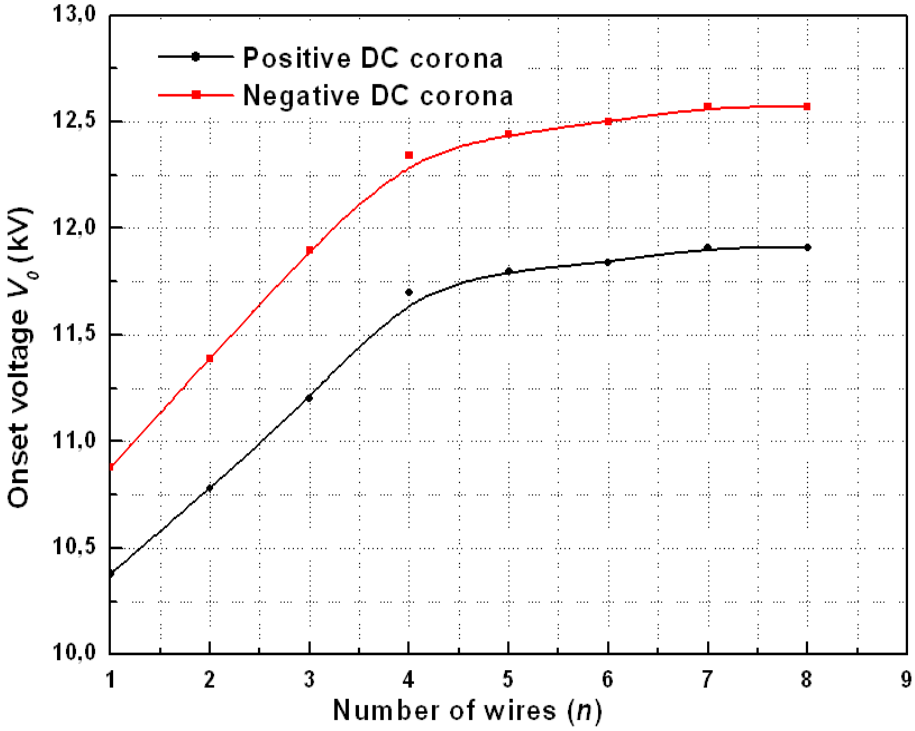

Fig. 6. Onset corona voltage versus the number of discharging wires.

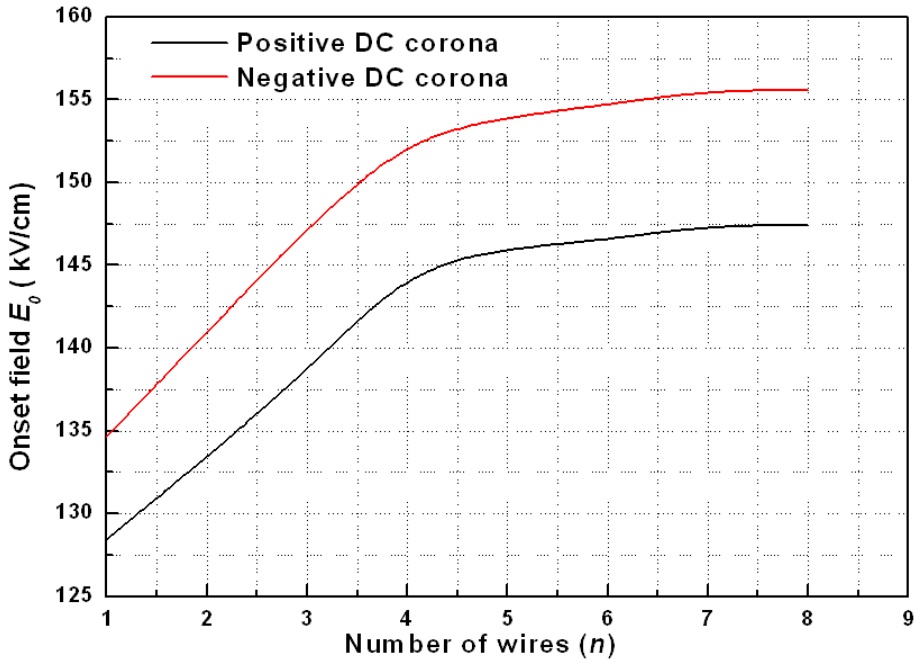

Fig. 7. Onset corona field versus of the wires number.

We note that from five wires (5W-ESP), the characteristics are stable regardless of the polarity of the applied voltage. The electric onset voltage and electric onset field of negative polarity are greater slightly than that of the positive polarity. From a certain

voltage V_C (breakdown voltage), we enter in the area of disruptive discharges with the presence of sparks or possibly an electric arc. We see in figure 8 that the breakdown voltage V_C is stable regardless of the number of wires of the active electrode. This voltage is higher against in a negative discharge. Therefore, the gap $(V_C - V_0)$ is often greater in a negative discharge, figure 9. For this reason, in the majority of ESPs, the discharge electrodes are supplied with a negative voltage to ensure the particle charge, electric field sufficiently intense as to minimize the strains.

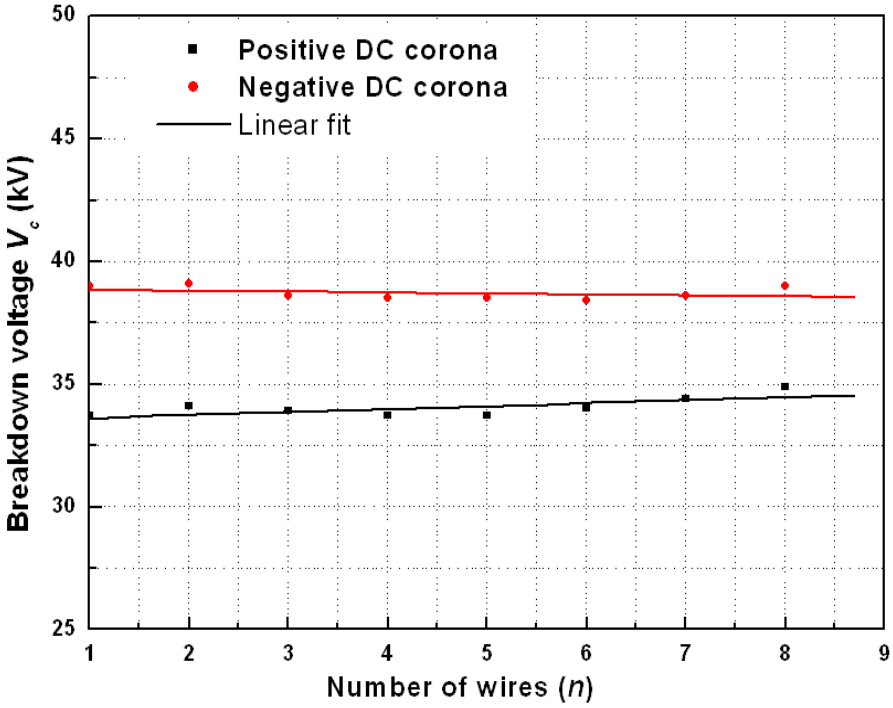

Fig. 8. Breakdown voltage versus the number of discharging wires.

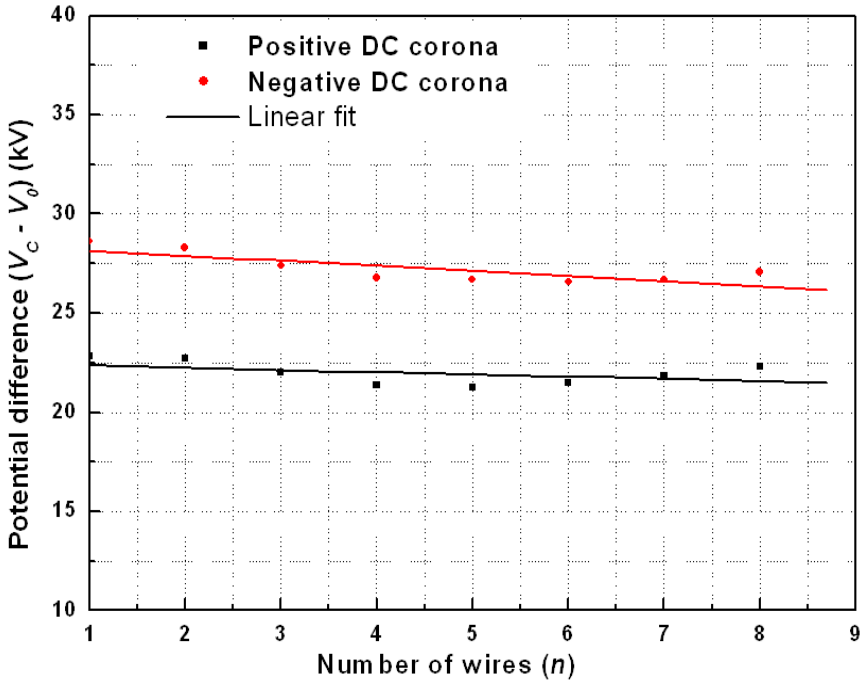

Fig. 9. Potontial difference according to a number of wires.

3.3 dimensional constant *A*

The figure 10 shows the dependence (I/V) as a function of $(V - V_0)$ and shows good linear behavior. In this case, the inception voltage obtained by extrapolating the right axis $(V - V_0)$ are positive, this formula does not lose its physical meaning. The parameter A can be determined by the slope of the characteristic $(I/V) = f(V - V_0)$ [13]. Dimensional constant A shown in figure 11, which is proportional to the apparent mobility of the charge carriers, is lower in the case of a positive polarity. In addition, it seems that the apparent mobility increases with the number of cases irrespective wires, which confirms the observation noted in the previous section.

The ratio of the dimensional constant $(A-/A+)$ is independent of the number of wires as shown in figure 12. The ratio is found to be a linear function of the number of wires. The value of the ratio $(A-/A+)$ gives the ratio $(\mu-/\mu+)$ the mobility of negative ions on the mobility of positive ions [21]. The value obtained can be regarded as constant in the present context $(A-/A+) \approx (\mu-/\mu+) \approx 1.085$.

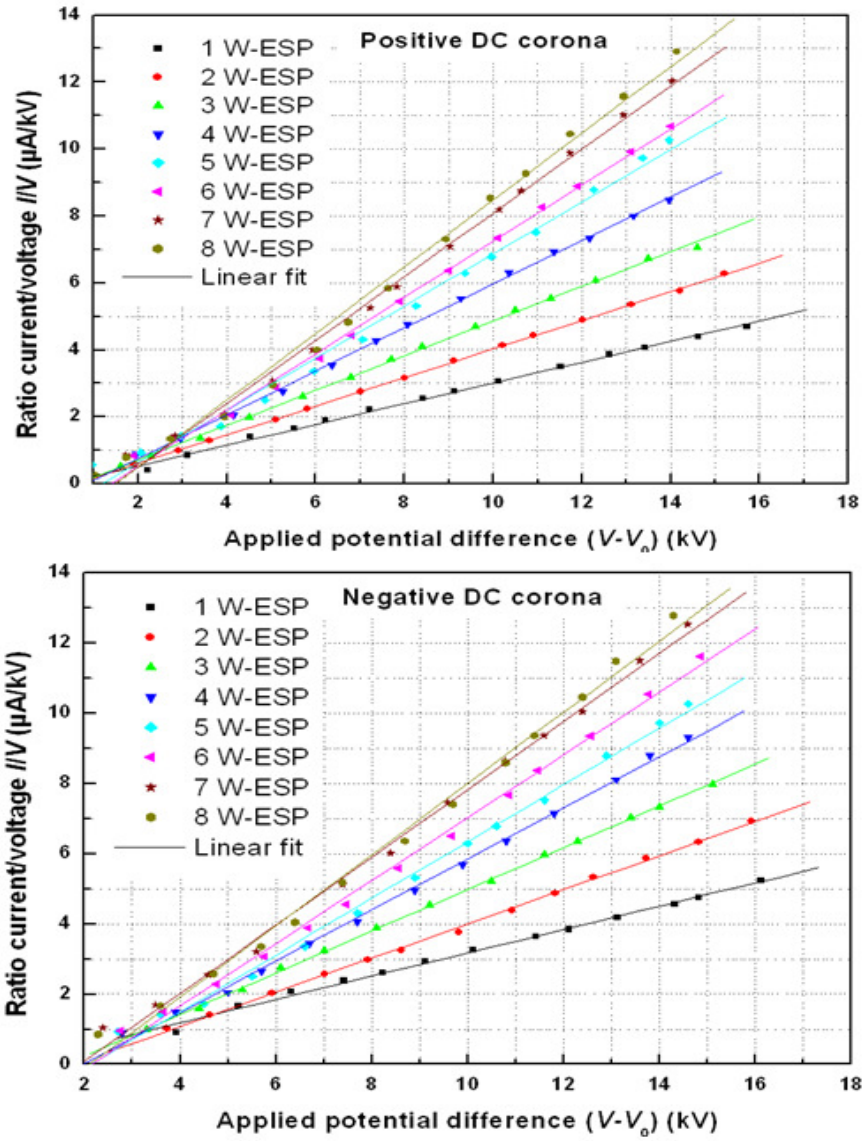

Fig. 10. The dependence of the current/voltage ratio (*I/V*) on the voltage difference $(V - V_0)$

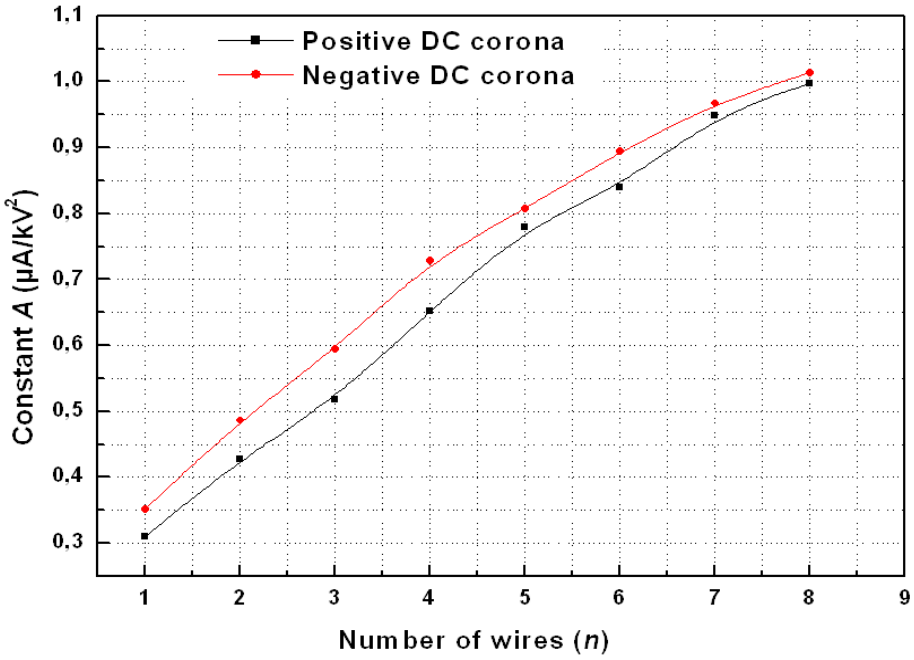

Fig. 11. Variation of the dimensional constant A with the number of wires.

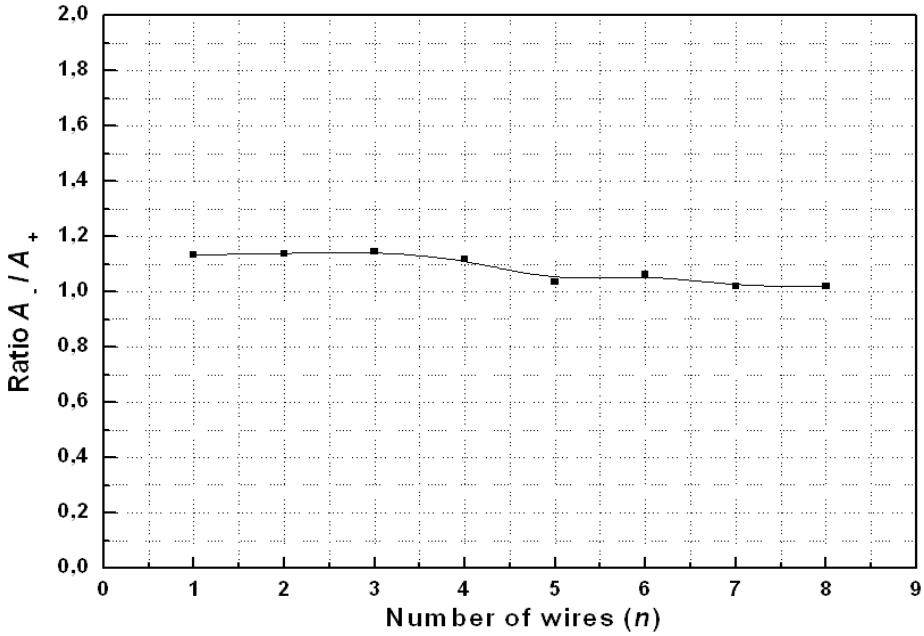

Fig. 12. Variation of the ratio $A-/A+$ according to a number of wires .

4. Mobility of charge carriers

From the classical formula originally obtained by Townsend and Thomson [14, 22], the current-voltage characteristic for a duct can be derived as [23, 24]:

$$I = \frac{4\pi\varepsilon_0\mu * l}{h^2 \log\left({}^{d}/_{r_0}\right)} V(V - V_0) \quad (5)$$

This formula requires that one be able to compute the constant d, a somewhat formidable task. However, this difficulty can be avoided for it can be shown that the following approximations are valid to within 1% under the conditions indicated.

For $\frac{h}{a} \leq 0.6$ $\quad d = \frac{4h}{\pi}$ (6)

For $\frac{h}{a} \geq 2.0$ $\quad d = \frac{a}{\pi} e^{\frac{\pi h}{2a}}$ (7)

In a duct precipitator, the current-voltage characteristic is given by equation 5 where the constant d is given by equation 7 because in our system $(h/a) = 2.5$, for a fixed wire-to plate spacing $h = 50mm$ and a fixed wire-to-wire spacing $2a = 40mm$, equation 6 states that the length d is independent of the wire-to-wire spacing this means that the corona current of wire does not depend on the wire-to-wire spacing until the wires approach each other very closely. The threshold voltage V_0 is given by $(I^{1/2}) = f(V)$ [20]. Mean value of ionic mobility was calculated from averaging the slop obtained from the least square analysis of (I/V) versus $(V - V_0)$ (see figure 9).

Figure 13 shows the value of ionic mobility as a function of the number of wires at pressure $P = 760mmHg$, temperature $T = 29°C$ and humidity $Hr = 65\%$. For 5W-ESP to 8W-ESP, the mobility of positive and negative charge carriers is independent with the number of wires. On the other side for 1W-ESP to 4W-ESP the ionic mobility increases with number of wires in both polarities.

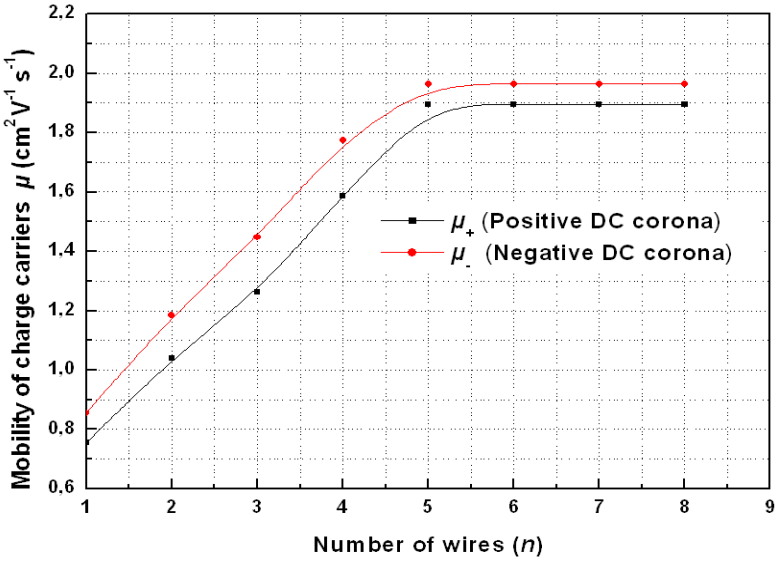

Fig. 13. The apparent mobility of the charge carriers by function of wires number.

5. Current density in the system

A formula for current density J as a function of the applied voltage V will be given for this geometry [25]:

$$J = \frac{2\pi\varepsilon_0\mu * l}{ah^2 \log\left(\frac{d}{r_0}\right)} V(V - V_0) \quad (8)$$

A modification of this formula is found when particles are present in the gas stream. The formula is to be applied using the absolute value of the voltage. However, the formula is valid for positive and negative polarity, provided an account is taken of the differing ion mobilities. Figures 14-15 show that the current density as a function the applied voltage for both polarity. The current density-applied voltage characteristic is a quadratic low whatever the nature of the polarity [26, 27].

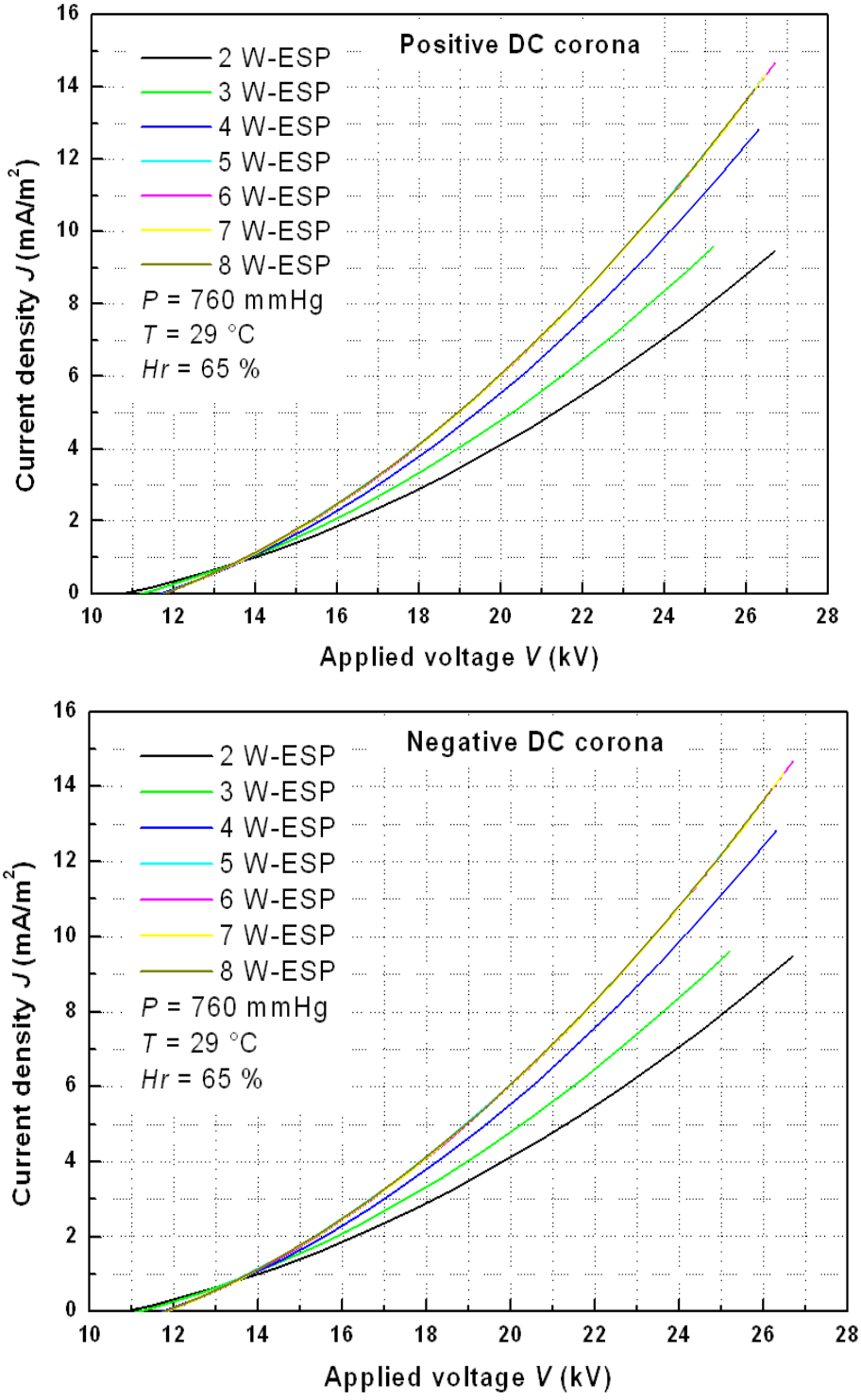

Fig. 14. Variation of the orona current density with the wires number.

6. Conclusion

The measurement of current-voltage characteristics of the corona discharge is the best way to characterize the electrostatic precipitator's types wire-to-planes and multi wires-to-planes. The experimental results have confirmed some aspects of this configuration and show that the variation of the current intensity as a function of applied voltage for different ESP is in good agreement with the classical law current-voltage made by Townsend. For a large number of wires electrostatic precipitator, the onset voltage and the onset field become independent of the number of wires whatever the nature of the polarity.

Based on the experimental data and the knowledge of corona inception, a new general formula was developed by Meng et al. for uncover the phenomena in point-to-plane geometry corona discharges. This formula can be apply in wires-to-planes system of an electrostatic precipitators because the scope of m is deduced in a range 1.5-2.0 and further confirmed with the results in earlier studies.

For the same gas and the same external conditions, the value of the breakdown voltage is much lower in positive polarity. The application voltage required to maintain the same discharge current is higher with positive polarity, and the corona onset voltage in a negative polarity is higher than that of the positive polarity. For this reason, in the majority of ESPs, the discharge electrodes are supplied with a negative voltage to ensure proper charging of particles, an electric field sufficiently intense as to minimize the strains.

The apparent mobility of the charge carriers increases with the wires number $n < 5$ for both polarity and the apparent mobility of positive corona is superior to negative corona. For $n \geq 5$, the ion mobility is independent of the wires number.

References

[1] J.S. Chang, A.J. Kelly, J.M. Crowley, Handbook of Electrostatics Processes, *Marcel Dekker, NewYork,* 1995.

[2] J.S. Chang, P.A. Lawless, T. Yamamoto, Corona discharge processes, *IEEE Trans. Plasma Sci.* 19 (1991) 1152–1166.

[3] I. Yamamoto, H.R. Velkoff, Electrohydrodynamics in an electrostatic precipitator, J. *Fluid Mech.* 108 (1981) 1-18.

[4] H. Nouri, N. Zouzou, E. Moreau, L. Dascalescu, Y. Zebboudj, Effect of relative humidity on current-voltage characteristics of an electrostatic precipitator, *J. Electrostat.* 70 (2012) 20-24.

[5] D.I. Carroll, I. Dzidic, R.N. Stillwell, K.D. Haegle, E.C. Horning, Atmospheric pressure ionization mass spectrometry: corona discharge ion source for use in a liquid chromatography- mass spectrometry-computer analytical system, *Anal. Chem.* 47 (1975) 2369-2373.

[6] M. Rickard, D. Dunn-Rankin, F. Weinberg, F. Carleton, Maximizing ion-driven gas flows, *J. Electrostat.* 64 (2006) 368-376.

[7] A. Mizuno, Electrostatic precipitation, *IEEE Trans. Dielectr. Electrostat. Insul.* 7 (2000) 615-624.

[8] J.S. Chang, Next generation integrated electrostatic gas cleaning systems, *J. Electrostat.* 57 (2003) 273-291.

[9] A. Jaworek, A. Krupa, T. Czech, Modern electrostatic devices and methods for exhaust gas cleaning: a brief review, *J. Electrostat.* 65 (2007) 133-155.

[10] B. Dramane, N. Zouzou, E. Moreau, G. Touchard, Electrostatic precipitation in wire-to-cylinder configuration: effect of the high-voltage power supply waveform, *J. Electrostat*. 67 (2009) 117-122.

[11] H. Nouri, Y. Zebboudj, Analysis of positive corona in wire-to-plate electrostatic precipitator, *Eur.Phys.J.Appl.Phys.*49 (2010) 11001.

[12] M. Aissou, H. Ait said, H. Nouri, Y. Zebboudj, Analysis of current density and electric field beneath a bipolar DC wires-to-plane corona discharge in humid air, *Eur.Phys. J.Appl.Phys.*61 (2013) 30803.

[13] R. Tirumala, Y. Li, D.A. Pohlman, D.B. Go, Corona discharges in sub-millimeter electrode gaps, *J. Electrostat*. 57 (2010) 1-7.

[14] J.S. Townsend, Electricity in Gases, *Oxford University Press, UK*. (1915) 375–376

[15] B.L. Henson, A space-charge region model for microscopic steady coronas from points, *J. Appl. Phys.* 52 (1981) 709.
[16] K. Yamada, An empirical formula for negative corona discharge current in point-grid electrode geometry, *J. Appl. Phys.* 96 (2004) 2472.
[17] G.F. Ferreira, O.N. Oliveira, J.A. Giacometti, Point-to-plane corona: corona–voltage characteristics for positive and negative polarity with evidence of an electronic component, *J. Appl. Phys.* 59 (1986) 3045.
[18] X. Meng, H. Zhang, J. Zhu, A general empirical formula of current–voltage characteristics for point-to-plane geometry corona discharges, *J. Phys. D: Appl. Phys.* 41 (2008) 065209.
[19] A. A. AZOOZ, S. I. WAYSI, An Alternative Empirical Formula for Positive Corona Discharge *I-V* Characteristics in Point-to-Plate Electrode Geometry, *Plasma Science and Technology*, 16 (2014) 211-218.
[20] M. F. Frechette, S. I. Kamel, DC corona discharge in SF6: Evidence of an electronic component for the negative polarity, *Proc. IEEE Int. Symp. on Electrical Insulation, Boston, USA,*1988.
[21] I. S. Wais, D. D. Giliyana, Sphere-to-plane electrodes configuration of positive and negative plasma corona discharge, *American Journal of Modern Physics,* 2 (2013),46-52.
[22] J. J. Thomson, G. P. Thomson, Conduction of electricity through gases, *Combridge University Press.* 2 (1933) 552-556
[23] P. Cooperman, A theory for space charge limited currents with application to electrical precipitation, *AIEE Trans.* 79 (1960) 47-50.
[24] P. Cooperman, Dust space charge in electrical precipitation, *AIEE Trans*. (1963) 324-326.
[25] G. Cooperman, A new current-voltage relation for duct precipitators valid for low and high current densities, *IEEE Trans.* 47 (1981) 236-239.
[26] H. Nouri, M. Aissou, Y. Zebboudj, Modeling and Simulation of the Effect of Pressure on the Corona Discharge for Wire–plane Configuration, *IEEE Transactions on Dielectrics and Electrical Insulation*,20(2013)1547-1553.
[27] B.Y. Guo, J. Guo, A.B. Yu, Simulation of the electric field in wire-plate type electrostatic precipitators*, J. Electrostat.* 72 (2014) 301-310.